

## Synthesis of $\text{Cd}_x\text{Zn}_{1-x}\text{S}$ Nanoparticles in Porous Vycor Glass by Reaction of Single-source Precursors

Yuji Wada,\* Daisuke Niinobe, Masahiro Kaneko, and Yasunori Tsukahara  
*Department of Material and Life Science, Division of Advanced Science and Biotechnology,  
 Graduate School of Engineering, Osaka University, 2-1 Yamadaoka, Suita, Osaka 565-0871*

(Received September 26, 2005; CL-051225; E-mail: ywada@mls.eng.osaka-u.ac.jp)

$\text{Cd}_x\text{Zn}_{1-x}\text{S}$  nanoparticles incorporated in a nanoporous Vycor glass (PVG) were fabricated by incorporating and decomposing bis(*N,N*-diethyldithiocarbamato)cadmium and bis(*N,N*-dibutyldithiocarbamato)zinc sequentially. Fabrication of the alloy compound was confirmed by the shift in the X-ray diffraction pattern with respect to those of pure CdS and ZnS.

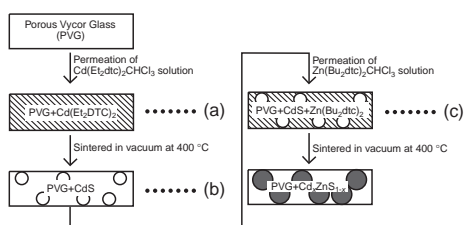
II–VI semiconductor nanoparticles have been attracting much attention for the application in optoelectric devices and photoelectric converters.<sup>1–3</sup> For tuning the emission wavelength and absorption spectrum of the particles, methods for tuning the size of the particles have been developed. Recently, as another approach for changing the absorption spectra of the particles, synthesis of alloy compound was extensively investigated because the band gap of alloy compounds can be easily modified by the composition of the compound.<sup>4</sup> For applying semiconductor nanoparticles to optical devices and photoelectric converters, it is necessary to incorporate particles into an appropriate porous medium or make composite with the particles and a matrix.<sup>5,6</sup> Therefore, methods for synthesizing nanocomposites have been investigated vigorously.<sup>7–10</sup>

For an approach to fabricating a composite material composed of alloyed nanoparticles in a porous medium, we present a novel method for synthesizing  $\text{Cd}_x\text{Zn}_{1-x}\text{S}$  nanoparticles in nanoporous Vycor glass (PVG, Corning 7930, mean pore diameter: 4 nm, thickness: 1.1 mm) by using the single-source precursor method.<sup>11,12</sup> The incorporation of molecular precursors into a porous medium is easier than that of particles because of the smaller size of the precursor molecules. Therefore, the single-source precursor method has an advantage in fabricating such composite materials: nanoparticles incorporated in porous medium.

The experimental procedure is presented in Scheme 1.  $\text{Cd}_x\text{Zn}_{1-x}\text{S}$  nanoparticles incorporated in PVG were synthesized by decomposing bis(*N,N*-diethyldithiocarbamato)cadmium ( $\text{Cd}(\text{Et}_2\text{dtc})_2$ ) and bis(*N,N*-dibutyldithiocarbamato)zinc ( $\text{Zn}(\text{Bu}_2\text{dtc})_2$ ) sequentially.  $\text{Cd}(\text{Et}_2\text{dtc})_2$  was synthesized according to the literatures.<sup>13</sup> Sodium *N,N*-diethyldithiocarbamate trihydrate

(10 mmol, 2.3 g) was dissolved in 10 mL of water.  $\text{Cd}(\text{NO}_3)_2 \cdot 4\text{H}_2\text{O}$  (5 mmol, 1.4 g) was dissolved in 2 mL of water. These solutions were mixed and the resulting white precipitate was filtrated. The filtrate was dried in vacuum. The product was characterized by  $^1\text{H}$  NMR, elemental analysis, and UV–vis spectroscopy. Anal. calcd for  $\text{C}_{10}\text{H}_{20}\text{S}_4\text{N}_2\text{Cd}$  (bis(*N,N*-diethyldithiocarbamato)cadmium): C, 29.30; H, 4.80; N, 6.80%. Found C, 29.41; H, 4.58; N, 6.87%. UV–vis ( $\text{CHCl}_3$ ,  $\lambda/\text{nm}$ ): 265, 285. The positions of the peaks in the absorption spectrum were same as those of the reported value.<sup>14</sup> The product was used as a precursor of CdS without further purification, and  $\text{Zn}(\text{Bu}_2\text{dtc})_2$  for the precursor of ZnS was purchased from TCI. A PVG was dipped in a 0.01 M trichloromethane solution of  $\text{Cd}(\text{Et}_2\text{dtc})_2$  for 1 h (Scheme 1a), and then was introduced in a glass tube and was degassed. The glass tube was heated at 100 °C in vacuum for 1 h to dry up the PVG and then was sealed. The glass tube was heated at 400 °C for 1 h to decompose  $\text{Cd}(\text{Et}_2\text{dtc})_2$  to produce CdS (Scheme 1b). The resulting PVG (PVG + CdS) was immersed in a 0.01 M trichloromethane solution of  $\text{Zn}(\text{Bu}_2\text{dtc})_2$  (Scheme 1c) and was introduced in a glass tube. The glass tube was heated at 100 °C in vacuum for 1 h and was sealed. The glass tube was then heated at 400 °C for 1 h to produce  $\text{Cd}_x\text{Zn}_{1-x}\text{S}$  alloy particles in PVG (PVG +  $\text{Cd}_x\text{Zn}_{1-x}\text{S}$ ). UV–vis absorption spectra of these PVGs were measured by a JASCO V-570 spectrophotometer.

For the characterization of the decomposed product of the precursors, X-ray diffraction (XRD) measurements were performed on the decomposed products of the precursors, which passed through almost the same procedure described above except that the precursor was not incorporated into PVG by solution. The sequential decomposition of  $\text{Zn}(\text{Bu}_2\text{dtc})_2$  followed by  $\text{Cd}(\text{Et}_2\text{dtc})_2$  with the same procedure described above was also performed and the XRD pattern was measured. XRD patterns of decomposed  $\text{Cd}(\text{Et}_2\text{dtc})_2$  and  $\text{Zn}(\text{Bu}_2\text{dtc})_2$  were also measured, respectively. The results are illustrated in Figure 1. It has been confirmed from the accordance of the patterns and the standard powder diffraction files that wurtzite hexagonal ZnS and CdS were successfully synthesized by decomposing the respective precursors (Figures 1a and 1b). Therefore, it can be considered that ZnS and CdS can be synthesized in PVG by decomposing the respective precursors incorporated in PVG. In the case of the sequential decomposition of  $\text{Cd}(\text{Et}_2\text{dtc})_2$  followed by  $\text{Zn}(\text{Bu}_2\text{dtc})_2$  (Figure 1d), the XRD peaks showed a large shift toward higher diffraction angle with respect to those of CdS. The shift of the peaks was attributed to the change in the lattice parameters by formation of  $\text{Cd}_x\text{Zn}_{1-x}\text{S}$ .<sup>4</sup> This was also supported by a report that stacked CdS and ZnS layers formed  $\text{Cd}_x\text{Zn}_{1-x}\text{S}$  by annealing at 400 °C.<sup>15</sup> The lattice parameter *c* estimated from the peaks in Figure 1d was 6.4 Å. It is well known that the lattice parameters of  $\text{Cd}_x\text{Zn}_{1-x}\text{S}$  shift in proportion to the ratio of Zn to



**Scheme 1.** Experimental procedure for fabricating  $\text{Cd}_x\text{Zn}_{1-x}\text{S}$  nanoparticles in PVG.

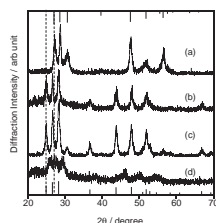


**Figure 1.** XRD patterns of the products after decomposing (a)  $\text{Zn}(\text{Bu}_2\text{dtc})_2$ , (b)  $\text{Cd}(\text{Et}_2\text{dtc})_2$ , (c)  $\text{Zn}(\text{Bu}_2\text{dtc})_2$  followed by  $\text{Cd}(\text{Et}_2\text{dtc})_2$ , and (d)  $\text{Cd}(\text{Et}_2\text{dtc})_2$  followed by  $\text{Zn}(\text{Bu}_2\text{dtc})_2$ . The vertical lines on the top and bottom of the figure indicate the standard powder diffraction patterns of wurtzite CdS (lower) and wurtzite ZnS (upper).

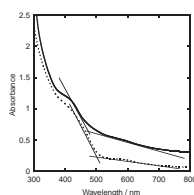


**Figure 2.** Absorption spectra of PVG + CdS (dotted line), and PVG +  $\text{Cd}_x\text{Zn}_{1-x}\text{S}$  (solid line).

Cd following the Vegard's law. Therefore, the Zn mole fraction expected from the lattice parameter can be estimated to be 0.5.<sup>4</sup> On the other hand, in the case of the sequential decomposition of  $\text{Zn}(\text{Bu}_2\text{dtc})_2$  followed by  $\text{Cd}(\text{Et}_2\text{dtc})_2$ , the XRD pattern showed the summation of each CdS and ZnS patterns (Figure 1c). This means that each of CdS and ZnS nanoparticles was synthesized independently in this case.

The absorption spectra of PVG + CdS and PVG +  $\text{Cd}_x\text{Zn}_{1-x}\text{S}$  are illustrated in Figure 2. In these spectra, broad peaks at around 600 nm were observed. These peaks would be attributed to an organic residue caused by decomposition of the precursors. The shift in the absorption edge of the decomposed product in PVG +  $\text{Cd}_x\text{Zn}_{1-x}\text{S}$  with respect to that of PVG + CdS was observed, which was attributed to the formation of  $\text{Cd}_x\text{Zn}_{1-x}\text{S}$  from the XRD measurement. The approximate absorption edges of CdS and  $\text{Cd}_x\text{Zn}_{1-x}\text{S}$  were estimated from the extrapolation of absorption at 410 nm and the background as shown in Figure 2. The band gap of CdS in PVG was estimated to be 2.5 eV and that of the  $\text{Cd}_x\text{Zn}_{1-x}\text{S}$  in PVG was estimated to be 2.6 eV, respectively. The band gap of CdS in PVG was almost same as that of bulk CdS. This can be explained as follows. The average size of the CdS particles would be around 4 nm because the average size of the pores in PVG is 4 nm. And the increase in band gap by quantum size effect appears extensively below the size of 4 nm in the case of CdS.<sup>16–18</sup> Therefore, the band gap of CdS in PVG estimated from the absorption spectrum would be almost same as that of bulk one. Because the sintering temperature was higher than the melting points of the precursors, the precursors would melt in the pores of PVG at first, and then decompose via the liquid phase. Because the precursors would be hydrophobic, the precursors would be sphere shape rather than rods for minimizing the surface energy.

The molar fraction of Zn in  $\text{Cd}_x\text{Zn}_{1-x}\text{S}$  in PVG +  $\text{Cd}_x\text{Zn}_{1-x}\text{S}$  sample estimated from the band gap obtained from

Figure 2 was 0.12.<sup>19</sup> The smaller content of Zn in  $\text{Cd}_x\text{Zn}_{1-x}\text{S}$  in PVG +  $\text{Cd}_x\text{Zn}_{1-x}\text{S}$  sample than that of the sample for XRD measurement was mainly attributed to the smaller amount of the residual  $\text{Zn}(\text{Bu}_2\text{dtc})_2$  after evaporation of  $\text{Zn}(\text{Bu}_2\text{dtc})_2$  during heating up to 400 °C. On the other hand, the band gap of the product of the sequential decomposition of  $\text{Zn}(\text{Bu}_2\text{dtc})_2$  followed by  $\text{Cd}(\text{Et}_2\text{dtc})_2$  in PVG was almost same as that of CdS in PVG + CdS sample (not shown here). The difference in the band gaps between the products by the decomposition of  $\text{Cd}(\text{Et}_2\text{dtc})_2$  followed by  $\text{Zn}(\text{Bu}_2\text{dtc})_2$  and by the decomposition of  $\text{Zn}(\text{Bu}_2\text{dtc})_2$  followed by  $\text{Cd}(\text{Et}_2\text{dtc})_2$  was attributed to the difference of the products, which can be confirmed from the result of XRD measurements indicating the formation of  $\text{Cd}_x\text{Zn}_{1-x}\text{S}$  in the case of the sequential decomposition of  $\text{Cd}(\text{Et}_2\text{dtc})_2$  followed by  $\text{Zn}(\text{Bu}_2\text{dtc})_2$  whereas individual CdS and ZnS in the case of the sequential decomposition of  $\text{Zn}(\text{Bu}_2\text{dtc})_2$  followed by  $\text{Cd}(\text{Et}_2\text{dtc})_2$ .

In conclusion, we have successfully synthesized  $\text{Cd}_x\text{Zn}_{1-x}\text{S}$  nano-particles in a nanoporous glass by sequential incorporation and decomposition of these precursors.

## References

- 1 M. Bruchez, Jr., M. Moronne, P. Gin, S. Weiss, A. P. Alivisatos, *Science* **1998**, *281*, 2013.
- 2 W. C. W. Chan, S. Nie, *Science* **1998**, *281*, 2016.
- 3 R. Plass, S. Pelet, J. Krueger, M. Grätzel, U. Bach, *J. Phys. Chem. B* **2002**, *106*, 7578.
- 4 X. Zhong, Y. Feng, W. Knoll, M. Han, *J. Am. Chem. Soc.* **2003**, *125*, 13559; X. Zhong, S. Liu, Z. Zhang, L. Li, Z. Wei, W. Knoll, *J. Mater. Chem.* **2004**, *14*, 2790; Y. Li, M. Ye, C. Yang, X. Li, Y. Li, *Adv. Funct. Mater.* **2005**, *15*, 433.
- 5 M. Zayat, F. del Monte, *Adv. Mater.* **2003**, *15*, 1809.
- 6 T. Hirai, H. Okubo, I. Komasaawa, *J. Phys. Chem. B* **1999**, *103*, 4228; T. Hirai, H. Okubo, I. Komasaawa, *J. Mater. Chem.* **2000**, *10*, 2592.
- 7 S. Yano, T. Ito, K. Shinoda, H. Ikake, T. Hagiwara, T. Sawaguchi, K. Kurita, M. Seno, *Polym. Int.* **2005**, *54*, 354.
- 8 A. Zaban, O. I. Mičić, B. A. Gregg, A. J. Nozik, *Langmuir* **1998**, *14*, 3153.
- 9 K. Kamada, M. Tokutomi, N. Enomoto, J. Hojo, *J. Mater. Chem.* **2005**, *15*, 3388; N. Enomoto, J. M. Tang, M. Uehara, J. Hojo, *J. Ceram. Process Res.* **2000**, *1*, 88.
- 10 H. Lin, T. Jin, A. Dmytruk, T. Yazawa, *J. Am. Ceram. Soc.* **2003**, *86*, 1991; K. Kuraoka, H. Zhao, T. Yazawa, *J. Mater. Sci.* **2004**, *39*, 1879.
- 11 P. O'Brien, R. Nomura, *J. Mater. Chem.* **1995**, *5*, 1761; T. Trindade, P. O'Brien, *Chem. Mater.* **1997**, *9*, 523.
- 12 S. L. Cumberland, K. M. Hanif, A. Javier, G. A. Khitrov, G. F. Strouse, S. M. Woessner, C. S. Yun, *Chem. Mater.* **2002**, *14*, 1576.
- 13 A. Frigerio, B. Halac, M. Perec, *Inorg. Chim. Acta* **1989**, *164*, 149; O. F. Z. Khan, P. O'Brien, *Polyhedron* **1991**, *10*, 325.
- 14 G. St. Nikolov, N. Jordanov, I. Havezov, *J. Inorg. Nucl. Chem.* **1971**, *33*, 1059.
- 15 I. O. Oladeji, L. Chow, *Thin Solid Films* **2005**, *474*, 77.
- 16 P. Lianos, J. K. Thomas, *Chem. Phys. Lett.* **1986**, *125*, 299.
- 17 T. Vossmeier, L. Katsikas, M. Gienig, I. G. Popovic, K. Diesner, A. Chemseddine, A. Eychmüller, H. Weller, *J. Phys. Chem.* **1994**, *98*, 7665.
- 18 P. E. Lippens, M. Lannoo, *Phys. Rev. B* **1989**, *39*, 10935.
- 19 R. Hill, *J. Phys. C: Solid State Phys.* **1974**, *7*, 521.